Neural Computing and Applications

Show, Tell and Summarise: Learning to Generate and Summarise Radiology Findings from Medical Images

--Manuscript Draft--

Manuscript Number:	NCAA-D-20-00864
Full Title:	Show, Tell and Summarise: Learning to Generate and Summarise Radiology Findings from Medical Images
Article Type:	Original Article
Keywords:	Medical Imaging; radiology report generation; Computer Vision; natural language processing
Abstract:	Radiology plays a vital role in healthcare by viewing the human body for diagnosis, monitoring, and treatment of medical problems. In radiology practice, radiologists routinely examine medical images such as chest X-rays and describe their findings in the form of radiology reports. However, this task of reading medical images and summarising its insights is time consuming, tedious, and error-prone, which often represents a bottleneck in the clinical diagnosis process. A computer-aided diagnosis system which can automatically generate radiology reports from medical images can be of great significance in reducing workload, reducing diagnostic errors, speeding up clinical workflow, and helping to alleviate any shortage of radiologists. Existing research in radiology report generation focuses on generating the concatenation of the findings and impression sections. Also, existing work ignores important differences between normal and abnormal radiology reports. The text of normal and abnormal reports differs in style and it is difficult for a single model to learn both the text style and learn to transition from findings to impression. To alleviate these challenges, we propose a Show, Tell and Summarise model that first generates findings from chest X-rays and then summarises them to provide impression section. The proposed work generates the findings and impression sections separately, overcoming the limitation of previous research. Also, we use separate models for generating normal and abnormal radiology reports which provides true insight of model's performance. Experimental results on the publicly available IU-CXR dataset show the effectiveness of our proposed model. Finally, we highlight limitations in the radiology report generation research and present recommendations for future work.

Powered by Editorial Manager® and ProduXion Manager® from Aries Systems Corporation

Manuscript

Click here to view linked References

Click here to access/download;Manuscript;manuscript_v7_19April.tex

Neural Computing and Applications manuscript No.
(will be inserted by the editor)

Show, Tell and Summarise: Learning to Generate and Summarise Radiology Findings from Medical Images

Sonit Singh · Sarvnaz Karimi · Kevin Ho-Shon · Len Hamey

Received: date / Accepted: date

Abstract Radiology plays a vital role in healthcare by viewing the human body for diagnosis, monitoring, and treatment of medical problems. In radiology practice, radiologists routinely examine medical images such as chest X-rays and describe their findings in the form of radiology reports. However, this task of reading medical images and summarising its insights is time consuming, tedious, and error-prone, which often represents a bottleneck in the clinical diagnosis process. A computer-aided diagnosis system which can automatically generate radiology reports from medical images can be of great significance in reducing workload, reducing diagnostic errors, speeding up clinical workflow, and helping to alleviate any shortage of radiologists.. Existing research in radiology report generation focuses on generating the concatenation of the findings and impression sections. Also, existing work ignores important differences between normal and abnormal radiology reports. The text of normal and abnormal reports differs in style and it is difficult for a single model to learn both the text style and learn to transition from findings to impression. To alleviate these challenges, we propose a *Show, Tell and Summarise* model that first generates findings from chest X-rays and then summarises them to provide impression section. The proposed work generates the findings and impression sections separately, overcoming the limitation of previous research. Also, we use separate models for generating normal and abnormal radiology reports which provides true insight of model's performance. Experimental results on the publicly available *IU-CXR* dataset show the effectiveness of our proposed model. Finally, we highlight limitations in the radiology report generation research and present recommendations for future work.

Keywords Medical imaging · radiology report generation · chest X-rays · computer-aided report generation · artificial intelligence · computer vision · natural language processing · deep learning.

Sonit Singh
Department of Computing, Macquarie University
Sydney, Australia
E-mail: sonit.singh@hdr.mq.edu.au

Sarvnaz Karimi
Data61, CSIRO
Sydney, Australia
E-mail: sarvnaz.karimi@data61.csiro.au

Kevin Ho-Shon
Department of Clinical Medicine, Macquarie University
Sydney, Australia
E-mail: kevin.ho-shon@mq.edu.au

Len Hamey
Department of Computing, Macquarie University
Sydney, Australia
E-mail: len.hamey@mq.edu.au

1 Introduction

Artificial Intelligence (AI) is one of most disruptive technologies to a majority of industries, including healthcare [1]. Medical imaging plays a vital role in healthcare by viewing the human body for diagnosis, monitoring, and treatment of medical conditions. In radiology practice, radiologists routinely examine medical images and conclude their findings in the form of radiology reports. These textual reports narrate the findings of the abnormalities and diseases present in the medical image. Figure 1 shows a sample chest X-ray with its accompanying radiology report. A radiology report consists of several sections, mainly *comparison*, *indication*, *findings* and *impression*. Examining medical images and writing radiology reports consume most of a radiologists' time. The task of examining medical images and

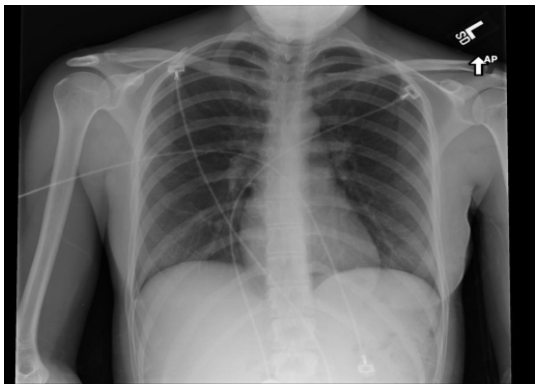

Comparison:
None.
Indication:
Chest pain, feels out of it.
Findings:
The Cardiomediastinal silhouette and pulmonary vasculature are wining normal limits in size. The lungs are clear of focal airspace disease, pneumothorax, or pleural effusion. There are no acute bony findings.
Impression:
No acute cardiopulmonary findings.

Fig. 1 An example of a chest X-ray and its corresponding radiology report in the IU-CXR dataset [2].

writing radiology reports is tedious, time consuming, error-prone, often representing a bottleneck in clinical diagnosis process. Also, with improvements in imaging techniques and the wider availability of imaging facilities, there is an increasing demand for imaging studies, resulting in clinical overload. Due to this, numerous scans remain unreported, leading to delayed or missed diagnoses and an adverse impact on patient care.

Computer-Aided Detection (CADe) and Computer-Aided Diagnosis (CADx) systems have been an integral part of the Picture Archiving and Communication Systems (PACS) for medical image analysis. These CAD systems plays a vital role in radiology practice by providing a second opinion, reducing labour cost, automating tedious and repetitive tasks, and helping alleviate the situation where the number of experienced medical experts is far below the demand. With the same goal to support radiologists, the task of automatic radiology report generation from medical images is proposed [3, 4, 5]. A CAD system which can automatically generate radiology reports from medical images can be great significance in reducing workload, reducing diagnostic errors, speeding up clinical workflow, and help in alleviating the situation where the number of radiologists are lower and medical resources are scarce.

Existing research [5, 6, 7] concatenates the findings and impression sections to form the target for radiology report generation task. This method lacks the ability to distinguish the heterogeneous information present in the actual radiology reports. The *findings* section is a detailed description of various pathologies, their location, and their severity. On the other hand, the *impression* section is a summary of the radiology report and concludes the radiology study. Hence, concatenating findings and impression section into a single text for radiology report generation is not a clear indication of a model's performance, given different nature of the two sections.

Previous research [5, 6, 7] trains a single model for radiology report generation from medical images irrespective of whether the images are normal or abnormal. A single model trained with both *normal* and *abnormal* radiology studies biases the model's performance towards generating normal reports given that abnormal studies are rare compared to normal studies. For example, in the IU-CXR data, about 2/3 of radiology reports are normal. Further, training of the single model gives equal weight to both normal and abnormal report studies, ignoring the fact that finding abnormalities and pathologies in medical images is critical in terms of clinical accuracy. Hence, results obtained from a single trained model are not reflective of whether the underlying learning model is able to successfully generate abnormal findings.

The task of medical image captioning aims to generate radiology reports that are coherent despite also being long. The concatenation of the findings and impression sections into a single text for radiology report generation increases the length of the text to generate, which deteriorates the performance of generation models. For example, research has shown that Recurrent Neural Networks (RNNs) have difficulty in modelling long-range dependencies [8]. Generating the findings and impression sections separately will help the model to improve its performance.

To alleviate limitations of the previous work, we propose a *Show, Tell and Summarise* model based on radiology report generation from medical images. A block diagram of our proposed model is shown in Figure 2. Our proposed model consists of three sequential modules: (1) an *image classification module* which classifies an input chest X-ray as *Normal* or *Abnormal*; (2) a *findings generation module*, which is an *encoder-decoder* framework [9] that takes either normal or abnormal chest X-ray as an input and generates *findings* as an output; and, (3) a *summarisation module*, which summarises the generated *findings* and gives an *impression* section as an output. We evaluate the proposed model on the publicly available Indiana University Chest X-ray Collection (IU-CXR) [2] dataset. The experimental

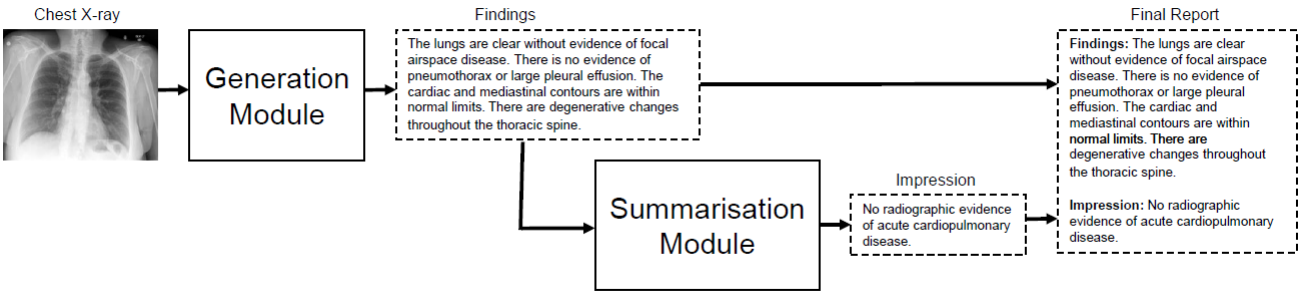

Fig. 2 Block diagram of show-attend-summarise model for generating and summarising radiology findings from medical images.

results show that the proposed model have capability to generate better findings and impression sections separately, given an input chest X-ray to the model.

The contributions of the paper are:

1. We present a novel architecture which can simultaneously classify a medical image, generate findings for a given medical image, and summarise the generated findings to form an impression of a radiology report;
2. We propose to model normal and abnormal reports separately, given that the linguistic characteristics of normal and abnormal reports are quite different in terms of syntactic and semantic information;
3. We propose to use *transfer learning* to solve the problem of relatively small-size annotated medical datasets. In particular, we use a CNN model pre-trained on the ImageNet dataset to initialise our CNN model. We also use pre-trained word embeddings such as *Glove* that are trained on large-scale corpora such as *Wikipedia* and *Common crawl* to initialise Long Short-Term Memory (LSTM) cells;
4. We propose to incorporate radiology domain knowledge by using RadGlove (Radiology Glove), pre-trained word embeddings that have been trained on 4.5 million radiology reports at Standford university; and,
5. We consider the generation of the *findings* and *impression* sections of radiology report separately in our proposed model. This helps overcoming challenges arising from concatenating findings and impression section as a single caption, which is one of the limitations of the previous work.

2 Related Work

In this section, we present background knowledge about standard deep learning models in medical image classification, image captioning, and summarisation systems, upon which our proposed model is based on. We also present an overview of related work in the radiology report generation from medical images.

2.1 AI in chest radiology

In recent years, due to the remarkable achievements of deep learning [10] in the field of computer vision, more and more deep learning techniques have been introduced in the field of medical imaging. AI has the potential of to transform the radiologists' workflow, carrying a positive knock-on effect for departmental efficiency as well as improved patient outcomes [11]. Success of deep learning techniques in healthcare heavily rely on the availability of large-scale annotated medical datasets. Naturally, radiology domain have large-scale medical data in the form of medical images and radiology reports, which is stored in hospital databases such as Picture Archiving and Communication Systems (PACS) for reviewing and organising images. The Radiological Information System (RIS) is also widely used for managing medical imaging data and the associated data. Apart from this, Electronic Health Records (EHR) is also growing due to wide interest for storing and organising clinical data including notes, pathology, and laboratory data.

Chest radiographs are one of the most widely used medical imaging modality in the world. With the release of large-scale medical datasets such as IU-CXR [2], ChestX-ray14 [12], PadChest [13], MIMIC-CXR [14], and CheXpert [15], research has started towards applying various classification networks in diagnosing pathologies on chest radiographs. Wang *et. al.* [12] applied pre-trained AlexNet [16], GoogLeNet [17], and ResNet-50 [18] to classify 8 disease categories. Guendel *et. al.* [19] proposed a local aware dense network for classification of 14 pathology classes in the ChestX-ray14 dataset. Rajpurkar *et. al.* [20,21] proposed CheXNet, a 121-layer CNN trained on the ChestX-ray14 for the pneumonia detection, which exceeds average radiologist per-

formance. Baltruschat *et. al* [22] proposed a fine-tuned ResNet-50 network which achieved high accuracy on 4 out of the 14 disease classes in the Chest X-ray dataset. Yao *et. al.* [23] presented a partial solution to constraints in using LSTMs to leverage inter-dependencies among target labels in predicting 14 pathological classes from Chest X-rays.

2.2 Medical image classification

One of the most fundamental tasks in computer vision and pattern recognition is *image classification*. Medical image classification aims at classifying a biomedical image as normal or abnormal, or assigning multiple disease labels. It may also refer to classifying an abnormality as benign or malignant, or assigning labels showing the severity of a lesion. Two main approaches in medical image classification are: (1) use of conventional handcrafted features such as Local Binary Pattern (LBP), Scale-Invariant Feature Transform (SIFT), Speeded Up Robust Features (SURF), and Bag of Visual Words (BoVW); and (2) use of automated features using deep learning techniques. Singh *et. al.* [24] did comparison of conventional features and deep learning features for modality classification and concept detection in medical images. They found that features extracted by CNNs using transfer learning outperform conventional handcrafted features. In [25], Wang *et. al.* showed that fine-tuning CNN models improves accuracy of CNN model for liver lesion classification. Using pneumonia detection task, Yadav *et. al.* [26] showed that using transfer learning and data augmentation, the accuracy of CNN models can further be improved. Zhang *et. al.* [27] proposed synergic deep learning, which use multiple CNNs simultaneously to mutually learn from each other for medical image classification. Kumar *et. al.* [28] introduced ensemble CNN model for medical image classification. In order to evaluate the performance of existing deep neural network for various medical image classification tasks, Faes *et. al.* [29] did a feasibility study by applying existing deep learning architecture to classify common diseases on five different datasets. Their results demonstrate that these automated algorithms have capability to show performance at par with state-of-the-art methods, and these methods can be used by healthcare professionals with no coding experience.

2.3 Image Captioning

The task of image captioning [9] aims at understanding the image and providing a natural language description of the image as an output. Image captioning is gaining its attention in both computer vision and natural language processing community due to its multi-modal nature. Image captioning is challenging because it not only requires the syntactic and semantic understanding of the language, but also need to understand scene type, location, object properties, and their interactions [30]. Image captioning have various applications including interaction of computers with humans, child education, health assistant for elderly care, and providing aid to visually-impaired people.

Research in image captioning falls under three main categories, namely *template based*, *retrieval based*, and *generation based* methods. Template-based approaches have fixed templates with a number of blank slots to generate captions. In this approach, first different objects, attributes, and actions are detected and then blank spaces in templates are filled. Farhadi *et. al.* [31] first extracted triplets of scene elements to fill the template slots for generating image captions. Li *et. al.* [32] proposed the method of first extracting phrases related to detected objects, attributes, and their relationships, and using this information for filling in the templates. To further extend this work, Kulkarni *et. al.* [33] adapted Conditional Random Fields (CRF) to infer objects, attributes, and propositions to fill gaps in sentence templates. Although template based methods are simple in terms of complexity, and can generate grammatically correct captions, these methods do not generate variable-length captions and lack in their capability to generate novel captions. Apart from this, template based methods have limitations that the rules are usually human-crafted and the generated sentences are usually rigid.

In retrieval based approaches [31,34,35,36], captions are retrieved from a set of existing captions. In this, given an input image, first visually similar images with their captions are find in the training set. The selected captions are called *caption pool or candidate captions*. The caption for the query image is selected from the caption pool. Farhadi *et. al.* [31] mapped images and descriptions to a common intermediate space for retrieving captions. Ordonez *et. al.* [36] proposed Im2Text model that utilises global image representations to retrieve and transfer captions from the dataset. Extractive summarisation methods were used to select the best caption for a given image. Hodosh *et. al.* [34] introduced Kernel Canonical Correlation Analysis (CCA) to project image and text to a a common space for caption retrieval. To alleviate impact of noisy visual estimation, Mason and Charniak [37] first find visual similarity images and retrieve a set of captions. They estimated a word probability density to score the existing captions

to select the best caption. Retrieval based methods produce general and syntactically correct captions. However, they cannot generate image specific and semantically correct captions. Also, retrieval based methods have limitations in terms of space search complexity due to selecting captions from a large caption pool.

With the rise of deep learning, neural network based methods become popular due to their tremendous performance on various computer vision and natural language processing tasks. These neural based methods first analyse the visual content of the image and then generate captions from the visual content using a language model which models the underlying context of captions. Neural based methods have the ability to generate novel captions that are semantically and syntactically more accurate than template and retrieval based methods. Kiros *et.al.* [38] proposed a multimodal language model that captures visual and linguistic context by CNN and LSTM. Inspired by the machine translation research, Vinyals *et. al.* [9] proposed an end-to-end framework for image captioning by combining CNN and LSTM models. Karpathy and Li [39] proposed a multimodal embedding model that aligns image and text modalities using CNN and LSTM models. Inspired by the natural human behaviour to pay attention to specific regions of image and then forming a good relationship of objects in those regions, *attention mechanism* was proposed by Xu *et. al.* [40] that finds salient regions in a image to describe content of an image. Liu *et. al.* [41] proposed novel model with different levels of explicit supervision for learning attention maps during training. This helps improving both the attention correctness and caption quality. It is found that not all words in a caption are associated with visual regions in an image. Hence, semantic concept words that are associated with image regions need to be learned but stop words are not associated with image regions. Various attention mechanism variants that take this into account are proposed by [42,43]. The traditional image captioning aims at describing an image with only a single sentence. However, one sentence's description is high-level and coarse. By only describing images with a single high-level sentence, there is a fundamental upper-bound on the quantity and quality of information approaches can produce [6,44]. Thus paragraph generation task is introduced, which aims to describe images in detail with a paragraph rather than a sentence [45].

2.4 Radiology Report Generation

Medical imaging has been an essential tool for clinicians to make diagnosis and deliver treatment. Radiologists routinely examine medical images and describe both normal and abnormal findings in the form of radiology report. Examining medical images is laborious and time-consuming because radiologists have to do lesion measurement and describe morphology for abnormalities. This task of examining medical images and writing textual radiology reports is time consuming, tedious, and often error-prone [46]. A radiology report consists of various sections including *comparison*, *indication*, *findings*, and *impression*. The findings and impression sections are the most important sections of a radiology report. The findings section is a paragraph containing multiple sentences that describe radiologists' observations about normal and abnormal regions present in an image. The impression section is a single-sentence summary or concluding remarks of a radiology study. An automated system that can generate radiology reports from medical images can benefit radiologists to focus more on other high-end complex cognitive tasks. With this ambition, researchers proposed the task of automated radiology report generation from medical images, also known as medical image captioning.

The goal of medical image captioning is to generate accurate, informative, complete, and coherent medical reports. This is a challenging task due to a number of reasons: (1) The generated report should correctly identify all the pathologies or abnormalities present in an image; (2) The generated report should be a long coherent paragraph that provides detailed description about findings in an image; and (3) The generated report should consists of heterogeneous information in the form of sections including *findings* and *impression* [47].

One of the early works integrating visual and linguistic data is towards leveraging radiology reports for medical image annotation in a weakly supervised manner. The detection of subtle disease characteristics using deep learning requires large amount of annotated medical data. Manual annotation of medical data is not scalable due to the requirement of experts, higher cost of annotation, time constraints, and also errors due to the subjective nature of human perception [48]. An alternative approach is to leverage the benefit of large-scale paired medical images-radiology reports data lying in hospitals' PACS. Schlegl *et. al.* [48] proposed the use of semantic content of textual radiology reports linked to the image data instead of voxel-wise annotations for training an image classifier. Their findings indicate that the inclusion of semantic representations got from radiology reports has advantage in improving classification accuracy of pathologies and learning semantic concepts such as spatial position. Shin *et. al.* [49] presented an interleaved text/image deep learning system to extract and mine the semantic interactions of radiology

images and reports from hospital's PACS. They mine disease terms from radiology reports using disease ontology and semantics and attach them to medical images, and demonstrate the prediction of the presence or absence of disease. Further, Shin *et. al.*[50] used large-scale radiology dataset to mine disease names and to used trained models to infer joint image/text contexts for composite image labeling.

One of the early works towards automated radiology report generation is by [3] where feature based approach is applied to predict categorical BI-RADS descriptors for breast lesions. Three main descriptors, namely, *shape*, *margin*, and *density* are used to train a classifier. Further categories for each feature are: **shape**: {*oval*, *round*, *irregular*}, **margin**: {*circumscribed*, *indistinct*, *spiculated*, *microlobulated*, *obscured*}, and **density**: {*nonhomogeneous*, *homogeneous*}. Although, the trained model can identify these features given a input image and fill them into a fixed template, the approach is limited to keywords and do not support coherent and free-form radiology report. Shin *et. al.*[50] used a cascaded CNN-RNN captioning model to generate description about the detected disease. Their model could generate individual words, however the generated words are not coherent and can be difficult to comprehend. This is due to the poor information extraction and language modelling capabilities. Later Zhang *et. al.* [51] proposed a CNN-RNN model enhanced by an auxiliary attention sharpening (AAS) module to automatically generate medical imaging report. They also demonstrated the corresponding attention areas of image descriptions. Their proposed model can generate more natural sentences but the length of each sentence is limited to 59 words. In addition, the content of a generated report is limited to five topics. Jing *et. al.* [5] proposed a hierarchical co-attention based model for generating medical imaging report. Their proposed model have capability to attend image features and predict semantic tags while exploring joint effects of visual and semantic information. Also, their model can generate long sentence descriptions in reports by incorporating a hierarchical Long-Short Term Memory (LSTM) network. However, they concatenated findings and impression section into a single text for generation task. Also, the experimental results show that their model was prone to generating false positives because of the interference of irrelevant tags.

Li *et. al.* [52] built a hierarchical reinforced agent, which introduced reinforcement learning and template based language generation method for medical image report generation. Their agent effectively utilise the benefit of retrieval and generation based approaches. However, the heavy involvement of pre-processing in extracting templates makes the method heuristic and difficult to generalise to other datasets and applications. Xiong *et. al.* [47] proposed a novel hierarchical neural network based Reinforced Transformer for medical image captioning (RTMIC) to generate coherent informative medical imaging report. The transformer module speeds up the training process by enabling parallel computing in feed-forward layers. Also, using bottom-up attention using pre-trained DenseNet model on ChestX-ray14 dataset that leads to more accurate pathological terminologies in the generated sentences. The use of reinforcement learning based training method addresses the discrepancy between Maximum Likelihood Estimation (MLE) based training objective and evaluation metrics of interest. However, only findings section was considered in the study and impression section is not included.

Yin *et. al.* [6] proposed a hierarchical recurrent neural network (HRNN) based medical report generation model. They also introduced a topic matching mechanism to HRNN, so as to make generated reports more accurate and diverse. The HRNN consists of two RNNs, a sentence RNN and a word RNN. The sentence RNN takes detected abnormalities and the features maps extracted by the CNN as inputs, and then generates several topic vectors. Given a topic vector, the word RNN produces an appropriate sentence. However, the underlying assumption that most sentences are only related a single disease or part of the location of the medical image is wrong. Moreover, they concatenate findings and impression sections as single text and regard the combined text as the ground truth report. Zeng *et. al.* [53] proposed a coarse-to-fine ultrasound image captioning ensemble model that can generate description of ultrasound images. First an organ classifier detect organ present in an ultrasound and then a respective encoder-decoder framework generates report for respective organ.

2.5 Summarisation Systems

Automatic text summarisation refers to the task of condensing the documents into a shorter version having the salient information from the source document. Radev *et. al.* [54] define a summary as a text that is no longer than the original text(s) and conveys important information in the original text(s). The reduction of data accomplished by text summarisation allow users to identify and process relevant information more quickly and accurately. In healthcare, the amount of data in the form of biomedical literature and patient's health records is growing exponentially. It is difficult for clinicians and

clinical researchers to cope with this abrupt rise in information. Automatic summarisation systems can definitely help clinicians and researchers to obtain a summary of a long single document or multiple documents [55]. Hence, text summarisation is an important tool to assist clinicians and researchers with their information and knowledge management tasks.

Existing summarisation approaches fall into three categories: *extractive*, *abstractive*, and *hybrid*. Extractive approaches select spans of text from the input text and copy them directly into the summary. Early non-neural techniques utilise domain expertise to develop heuristics for content select [56,57,58]. On the other hand, more recent neural based techniques allow for end-to-end training for text summarisation. Abstractive approaches paraphrase the source documents and create summaries with novel phrases not present in the source document [59]. Most of the research in abstractive summarisation use attention and copying mechanism [60,61,62]. Hybrid approaches is the mix of extractive and abstractive approaches, where first salient sentences are selected using extractive approach and then paraphrasing is done to get novel sentences using abstractive approach [63,64,65,66]. To address the limitation that neural models with a fixed vocabulary can not handle out-of-vocab words, a pointer-generator is used to copy elements directly from the input sequence [67]. To overcome the issue of repetition in the generated summaries, a coverage mechanism was proposed [60].

3 Methodology

In this section, first we define the task and provide a detailed description about our proposed *show, tell and summarise* model. Since annotated medical datasets are of small size, we use pre-trained models that are trained on large-scale annotated datasets to apply knowledge and skills learned from large-scale generic datasets to small size medical datasets.

3.1 Task Definition

The first module is an *image classification module*, which classifies an input chest X-ray as normal or abnormal. The image classification module is a binary classification problem where the input is a chest X-ray I and the classifier predicts the labels, $l = \{0, 1\}$, where 0 represents *normal* and 1 represents *abnormal*.

The second module is a *generation module*, which is an *encoder-decoder* framework. It first extracts the global image features using CNN and then fed into an LSTM for generating sequence of words, which forms the *findings* for the input chest X-ray. For generating radiology findings from chest X-rays, we are given an input image I and the model should generate a sequence of words $\mathbf{y} = (y_1, y_2, \ldots, y_N)$, where y denotes the description in the form of a radiology findings and $y_1 \ldots y_N$ denote words in the findings. Given a training set $D = (I, y)$ which consists of (I, y) pairs, where I represents a given medical image and y represents an accompanied radiology findings for the image in the form of $y = (y_1, y_2, \ldots, y_N)$, we train the model w.r.t its parameters θ in order to maximise a probabilistic model $p_\theta(y_1, y_2, \ldots, y_N|I)$.

The third module is a *summarisation module*, which takes findings generated by the generation module and summarises it to impression as an output. Given a paragraph of findings generated by the generation module which is represented as a sequence of tokens $p = \{p_1, p_2, p_3, \ldots, p_N\}$, where N is the number of tokens in the findings section, the summarisation module find a sequence of tokens $q = \{q_1, q_2, q_3, \ldots, q_L\}$ that best summarises the salient and clinically significant findings in p, where L is an arbitrary length of the summary or impression section. Since, we do have *findings-impression* pairs in our dataset, we can train a summarisation module in the form of supervised learning.

3.2 Model

The detailed architecture of our *show, attend and summarise* model is shown in Figure 3.

3.2.1 Image classification module

The goal of the image classification module is to classify an input Chest X-ray into normal or abnormal. The image encoder is a Convolutional Neural Network (CNN) that automatically extracts hierarchical visual features from images. More specifically, we use Inception-v3 [17] model pre-trained on the large-scale ImageNet [68] dataset. We resize the input images to 299×299 to keep consistent with the pre-trained Inception-v3 model.

3.2.2 Findings generation module

The findings section is a paragraph having high-level description of the image. The goal of findings generation module is to take the global visual features learned by the image encoder as input and generates the findings as an output. For findings generation, a stacked LSTM is used for the decoding step. The LSTM cell has multiplicative gate structure that deals well with exploding

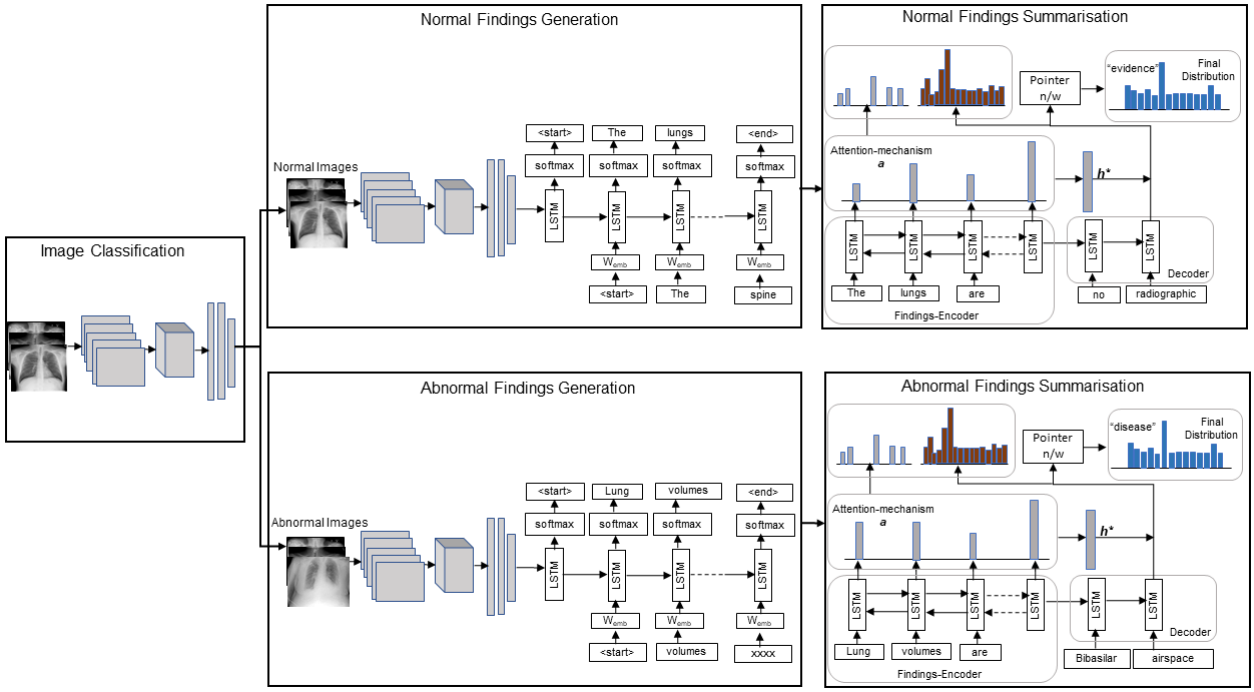

Fig. 3 Architecture of a Show, Tell and Summarise model for radiology report generation from medical images.

and vanishing gradient problem, and is a good solution to the problem of long-term sequence dependency. The visual feature vector is used as the initial input of the LSTM to predict the first word of the sentence and then the whole sentence is produced word by word. In our LSTM module, the dimensions of word embedding and the dimensions of hidden states are 300 and 1024 respectively.

3.2.3 Findings summarisation module

The goal of summarisation module is to summarise generated findings by the generation module. We use summarisation module proposed by Zhang *et. al.* [69]. The summarisation module is based on an encoder-decoder architecture that falls under the category of neural summarisation systems. The encoder learns hidden state representations of the input findings and the decoder decodes the input representation into an output sequence in the form of impression.

For the encoder, a Bi-directional Long Short-Term Memory (Bi-LSTM) network is used. Given the findings sequence in the form $p = \{p_1, p_2, p_3, \ldots, p_N\}$, p is encoded into hidden state vectors as given in equation 1.

$$h = Bi - LSTM(p), \tag{1}$$

where $h = \{h_1, h_2, \ldots, h_N\}$. The last hidden state h_N combines the last hidden states from both directions in the encoder.

After the entire sequence of findings is encoded, the output sequence is generated step by step with a LSTM decoder. The initial state of decoder is set to the last hidden state, *i.e.*, $s_0 = h_N$. At each t-th step, based on the previous generated token q_{t-1} and the previous decoder state s_{t-1}, the decoder calculates the current state s_t using equation 2.

$$s_t = LSTM(s_{t-1}, y_{t-1}), \tag{2}$$

In order to overcome the issue of information loss, an *attention mechanism* [70] which uses a weightage sum of all input states at every decoding step. Given the decoder state s_t and an input hidden state h_i, an input distribution a^t is calculated as:

$$e_i^t = v^T tanh(W_h h_i + W_s s_t), \tag{3}$$

$$a^t = softmax(e^t), \tag{4}$$

where W_h, W_s and v are learnable parameters. A weightage input vectors is calculated as:

$$h_t^* = \sum_i a_i^t h_i, \tag{5}$$

where h_t^* encodes the salient information which useful in the decoding step t. Finally, an output vocabulary distribution at step t is calculated as:

$$P(q_t|p, q_{<t}) = softmax(V^{'} tanh(V[s_t; h_t^*])), \tag{6}$$

where $V^{'}$ and V are learnable parameters.

In order to generate impressions which can leverage "copy" mechanism that can directly copy salient observations from input findings, a pointer-generator network is used. At each decoding step t, model can decide either to generate a word from the vocabulary with a generation probability p_{gen}, or copy a word directly from the input sequence with probability $1-p_{gen}$, where p_{gen} is model as:

$$p_{gen} = \sigma(w_{h*}^T * h_t^* + w_s^T s_t + w_q q_{t-1}), \quad (7)$$

where q_{t-1} denotes the previous decoder output, w_{h*}, w_s, and w_q are learnable parameters and σ is a sigmoid function. The overall output distribution in the pointer-generator network is:

$$P(q_t|p, q_{<t}) = p_{gen} P_{vocab}(q_t) + (1 - p_{gen}) \sum_{i:p_i=q_t} a_i^t, \quad (8)$$

where $P_{vocab}(q_t)$ is the same as the output distribution in equation 6.

3.3 Transfer Learning

Transfer learning [71] defines the ability of a system to recognise and apply knowledge and skills learned in previous tasks to a novel task. In transfer learning, the neural network is trained in two stages: (1) *pre-training*, where the network is generally trained on a large-scale benchmark dataset such as ImageNet [68], representing a wide diversity of labels or categories; and, (2) *fine-tuning*, where the pre-trained network is further trained on the specific target task of interest, which may have fewer labeled examples than the pre-training dataset [72]. The pre-training step helps the network learn general features than can be reused on the target task. Given a neural network, as the data propagates deeper through the network, the more specific features the network can extract. So, the initial layers detect basic features such as edges, colours, and shapes whereas the deeper layers learn more data-specific features. Hence, we can use a pre-trained model to detect the basic features using a large-scale annotated dataset and then add our customised layers to detect the data-specific features. It has also been observed that using pre-training weights results in faster convergence and this is due to significant feature reuse [72]. Transfer learning is beneficial when the data is not enough or training time and computing resources are restricted.

In this paper, we employ *transfer learning* to address the problem of relatively small medical image datasets. We use the pre-trained CNN model trained on the ImageNet dataset to initialise our encoder model. For the language generation and summarisation models, we initialise the LSTM with pre-trained word embeddings trained on large-scale corpora such as *common crawl*, and *Wikipedia*. In order to add medical domain knowledge, we use *Radglove* (Radiology Glove) word embeddings that have been originally trained on 4.5 million radiology reports at Stanford university.

4 Experimental Setup

In this section, we first describe about the dataset used for experiments and briefly describe various evaluation metrics to evaluate the proposed model. We then provide details about several model parameters that are set in model configuration.

4.1 Dataset

In order to evaluate the effectiveness of our proposed methodology, we did experiments on a publicly available dataset comprising medical images and associated reports, namely the Indiana University Chest X-ray collection (IU-CXR) [2]. The dataset is curated from 2 large hospital systems within the Indian Network for Patient Care databases. The IU-CXR dataset is publicly accessed through the Open Access Biomedical Image Search Engine (OpenI). There are 7,470 chest X-rays and 3,955 radiology reports. Majority of the studies have both frontal and lateral views of chest X-rays. Each radiology report consists of four sections, namely, *Comparison*, *Indication*, *Findings*, and *Impression*. The *comparison* section contains previous information about the patients' study, *i.e.*, any preceding medical exam with which current study is being compared to. The *indication* section contains symptoms of patients or reasons of examination, due to which study is being undertaken. The *findings* section lists the radiology observations. It provides detailed information about normal and abnormal regions in the medical image and its location in the image. The *impression* section summarises the findings section and concludes the radiology report. All reports are fully anonymised using de-identification techniques. About 2.5% of findings and impression words are also removed during anonymisation, resulting in some keywords missing in reports. Since the original data are from multiple hospitals and are inconsistent, there are some images or findings missing in the original dataset.

Our proposed model first generates findings from chest X-rays and then summarise the generated findings to get impression section. Hence, the overall pipeline is as follows: *CXR* $\longrightarrow$ *Findings* $\longrightarrow$ *Impression*. We consider *findings* for the generation task and then passing it to summarisation module to get final *impression* section. In the IU-CXR dataset, majority of reports don't

Table 1 Split of Normal Images and Abnormal Images into training, validation, and test sets.

	Normal	Abnormal
Data split	**# of images**	**# of images**
Training	4338	1423
Validation	250	100
Testing	250	100
Total	4838	1623

have *comparison* and *indication* sections, so we do not consider them in our study as prior work has also considered the same constraint. For our proposed model, we need both *findings* and *impression* section. We filtered out all reports which do not have both the findings and impression section. With this filtering, we are left with a reduced dataset of 6461 radiology reports. Since the impression section is the most indicative whether a scan is positive or negative and there is no labeled dataset, we applied *rule-based text processing* to classify a radiology report into either *Normal* (Negative) or *Abnormal* (Positive). Out of these, there are 4838 radiology reports that are *Normal* and 1623 are *Abnormal*. Table 1 shows the split of our dataset following the same distribution of previous studies [5,73].

For text processing, we tokenised all text and converted into lower case to map to a common vocab of 1,699 words. We removed numbers and special tokens, except full stop. We decided to drop infrequent words with less than 5 frequency. We also added two special tokens, <*start*> and <*end*> to indicate the start and the end of a sentence. To evaluate our models, we randomly shuffle our dataset and dividing into training, development, and testing. The split for the training, development, and testing set is shown in Table 1.

4.2 Evaluation Metrics

In order to evaluate the effectiveness of our proposed model, we use standard image captioning metrics, namely, BLEU [74], ROUGE [75], METEOR [76], and CIDEr [77], which originated from machine translation and summarisation. In order to check how effective impressions which are summarised from generated findings compared to the reference impressions, we use widely used summarisation ROUGE metric. We report results in the form of F_1 scores for ROUGE-1, ROUGE-2, and ROUGE-L, which measure the word-level unigram overlap, bigram overlap and the longest common sequence between the reference impressions and predicted impressions.

Bilingual Evaluation Understudy (BLEU), which is a standard evaluation metric for machine translation, and is also widely used in the evaluation of image captioning. BLEU analyses the correlation of n-grams between the generated text and the reference text. BLEU measures the word n-gram overlap between the generated and the ground truth caption. BLEU-1 considers unigrams, BLEU-2 consider bigrams, and so on. A brevity penality is added to penalise short generated descriptions. Recall-Oriented Understudy for Gisting Evaluation (ROUGE) counts the number of overlapping units such as n-grams, word sequences, and word pairs between the generated text and the reference text. ROUGE-L is the ratio of the length of the longest common sub-sequences between the machine-generated text and the reference text. Metric for Evaluation of Translation with Explicit ORdering (METEOR) calculates the harmonic mean of precision and recall. METEOR uses stemming, in particular, Porter stemmer and WordNet ontology to check for synonyms in the text. To take into account longer sub-sequences, it includes a penalty of up to 50% when no common n-grams exist between the machine-generated text and the reference text. METEOR demonstrated to have high levels of correlation with human judgements of translation quality. It has high correlation in the aspects of words, sentences, and subsections with human judgements. Consensus-based Image Description Evaluation (CIDEr) is a novel metric for evaluating image descriptions that uses human consensus. It measures the cosine similarity between n-gram TF-IDF representations of the two captions (words are also stemmed). This is calculated for unigrams to 4-grams and their average is returned as the final evaluation score. All evaluation metrics are implemented in COCO-evaluation code [78].

4.3 Model Configurations

All experiments are implemented in Python 2.7 using Keras [79] library with a Tensorflow [80] backend. Since training a deep neural network requires Graphics Processing Units (GPUs) to accelerate the computation process, we use two Nvidia Tesla P100 GPUs on a GPU cluster.

For the *image classification module*, we employed Inception-v3, a CNN model which is already trained on the ImageNet dataset and used it on chest X-rays from the IU-CXR dataset. The Inception-v3 model works as a multi-level feature extractor by computing 1×1, 3×3, and 5×5 convolutions. In order to use pre-trained Inception-v3 model, we resized images to 299×299. Images are normalised between 0 and 1 by dividing the raw pixel values by 255. We use *binary-crossentropy* as the

loss metric since we are solving a binary classification problem. We use Adam [81] optimiser with a learning rate of 0.0001.

For the *findings generation module*, we use an encoder-decoder framework which takes classified normal or abnormal chest X-ray as an input and generates normal or abnormal findings respectively. For the image encoding part, we use Inception-v3 which gives a 2048-dimensional vector as an output. In order to leverage transfer learning by using weights learned on the ImageNet, we process each Chest X-ray having dimensions of 299×299. For the generation part, the dimension of the LSTM output is set to 300. In order to leverage transfer learning on text data, we use *Glove* embeddings which are are 300-dimensional vectors and are given as an input to the LSTM for each word during training. In order to capture the radiology domain context, we use *RadGlove* embeddings providing an embedding of 100-dimension for each word. Instead of using a single LSTM as per our baseline model, we incorporate n-stage stacked LSTM, where $n = \{1, 2, 3\}$ to formulate a decoder which helps in learning rich semantic context of radiology reports during training. When initialising decoder with generic Glove embeddings, the dimensionalities of the word embedding space and the hidden state of LSTM are set to 300. For initialising decoder with RadGlove embeddings, the dimensionality of the word embedding space is set to 100 and the hidden state of LSTM is set to 300. The vocabulary is obtained by processing text of findings by turning words to lower case and removing words that are non-alphabet characters and appear less than 5 times. We train our model in an end-to-end manner by minimising our loss function using Adam algorithm with a *batch size* of 32. We set initial learning rate to 0.0005 which decays by a factor of 0.3 after 10 epochs, and the dropout rate is set to 0.2. Early stopping is used to prevent overfitting of the model. The best model configuration is selected based on the highest CIDEr score on the validation set. The experimental results in [82] report beam-search size of $l = 3$ produced the best results. Adapting their approach, during inference, we set beam-search of size 3 to generate radiology report for a given medical image.

For the *summarisation module*, we use an encoder-decoder framework based neural summarisation which is pre-trained on 4.5 million radiology reports at Stanford university [69]. In particular, a neural sequence to sequence model with copy mechanism is used to summarise findings to have conclusive summary or impression of a radiology report.

In order to use transfer learning, Glove [83] algorithm is applied to a corpus of 4.5 million radiology reports. The resulting 100-dimensional word vectors are used to initialise the word embeddings of seq2seq model. A 2-layer Bi-LSTM is used for encoders with their hidden size of 100 for each direction. The decoder is a 1-layer LSTM with its hidden size of 200. The negative log-likelihood loss is optimised using the Adam optimiser. A dropout of 0.5 is used to avoid the problem of overfitting models. Since impression is generally a single-sentence summary, the decoding is stopped whenever a $< EOS >$ token is predicted, otherwise it get stopped after generating maximum sequence length of 100. We use the official code implementation of summarisation model as available on the github repository of its original authors[1].

5 Quantitative Results

In this section, we provide results obtained for generating findings in terms of standard captioning metrics, namely, BLEU, CIDEr, METEOR, and ROUGE. We also provide results for the summarisation system comparing the predicted impression and the reference impression, in terms of ROUGE-1, ROUGE-2, and ROUGE-L metrics.

5.1 Results on generating radiology findings

Table 2 shows results for generating normal radiology findings given a normal chest X-ray to the findings generation module. Prior work considered concatenating findings and impression section as a single text for radiology report generation from chest X-rays. But in our study, we consider generating findings and impression section separately. Hence, no head to head comparison is possible with the previous work in terms of evaluation metrics. We implemented a vanilla CNN-RNN model, namely NIC model proposed by Vinyals *et. al.* [9] as a baseline model. We compare our proposed model and its variants with the baseline model. The higher value in all metrics represents better generated findings. All the reported results are on the *test* set and are computed by comparing the generated findings with their reference ones as given in our dataset. We observe that our proposed model outperforms the baseline model in all the evaluation metrics with a fair margin. Results show that initialising LSTM decoder with medical pre-trained text embeddings such as *RadGlove* is beneficial compared to random initialisation and initialising LSTM decoder with generic pre-trained embeddings that are trained on large-scale generic text.

[1] https://github.com/yuhaozhang/summarize-radiology-findings

Since, we aim to generate radiology findings from chest X-rays, RadGlove embeddings which are obtained by training Glove algorithm on a corpus of 4.5 million radiology reports is beneficial since it captures the domain knowledge and models the radiological language. It is worth noting that pre-trained Glove embeddings are 300-dimensional word vectors but RadGlove pre-trained embeddings are 100-dimensional word vectors. Various studies have found that larger embedding sizes helps to capture more context, but still RadGlove outperforms Glove embedding highlighting the importance of incorporating medical domain knowledge for radiology report generation task.

Table 3 shows results for generating reports on abnormal chest X-rays. On comparing results in Table 2 and Table 3, we clearly see that scores are lower for abnormal reports in terms of all evaluation metrics. This indicate that abnormal report generation is challenging compared to normal report generation. This is evident from the fact that normal reports are shorter than abnormal reports [73]. Also, if study is normal, radiologists do not provide detailed description in findings section and often summarise their study as normal in the impression section. On the other hand, if study is abnormal, radiologists need to write detailed description about normal and abnormal regions along with their location in chest X-rays. Apart from this, an abnormal radiology report contains many disease terms (or semantic terms) compared to a normal radiology report, making its generation more challenging.

5.2 Results on summarising radiology findings

One of the novelty of our proposed model is that we are generating findings and impression separately, which are sections of heterogeneous information and are required separately as in actual radiology practice. Table 4 shows the results for summarising the generated normal findings to get impression section for normal radiology report. In these set of experiments, we compare the generated summary with the reference summary [2]. Although, summarisation module takes in generated findings as input text and summarises it to provide impression as the generated text, we provide results for all the variants of the generation module to highlight how effective input findings are to the summarisation module, which lead to better summarised impression section. Experiment results show that our proposed model and its variants provide better results compared to the baseline model. From these results, we can also infer that better the generated findings are, the better is the summary from the summarisation module. On comparing results for generating summary of radiology findings on a private dataset at Stanford university [69], we can infer that the summarisation module is effective in summarising radiology findings to provide impression section of a radiology report.

Table 5 shows the results for summarising abnormal findings to get impression section fro an abnormal radiology report. From the results, we can infer that our proposed model helps in generating better impression. Comparing the results in Table 4 and Table 5, we can see a huge gap in scores of ROUGE-1, ROUGE-2, and ROUGE-L for summarising normal and abnormal radiology findings. The higher scores on summarising normal radiology findings and quite lower scores on summarising abnormal radiology findings indicate that model is good at generating normal impression section whereas it shows poor performance in generating abnormal impression section. On digging the reason for this performance, we find that normal impressions are generally a single phrase and there are few fixed templates which are repetitive in majority of normal reports and they are semantically similar in radiology context. For instance, Table 6 shows the most common templates for an impression section in a normal radiology report. These common impression templates for radiology report concludes that the radiology study is normal (Negative). It is important to note that most of these impression templates are single phrase and are semantically similar, which neural seq2seq model can easily learn.

On the other hand, the impression of an abnormal radiology report are rich in diversity in terms of disease terms and are much longer than their normal counterparts. Table 7 shows 3 representative impression sections of abnormal reports that are selected from the dataset. The first example shows *recommendation of followup study,* which is common if the radiology study is positive and need any additional study to confirm. The second example shows *conversation with physician* to discuss the nature of study. In third impression in Table 7 start with word *stable,* which is temporal in nature, indicating that the current study is compared with any previous study and found that cardiomegaly is stable in nature. Although, such sequential studies are often done in order to see the progression of disease, in the current dataset this will make language model to learn these words though we don't have any sequential studies, in turn generating spurious radiology reports.

[2] We interchangeably use summary or impression to denote conclusive remarks of a radiology report.

Table 2 Experimental results on generating radiology findings from normal medical images in terms of BLEU-n (n=1,2,3,4), CIDEr (C), METEOR (M) and ROUGE (R) scores on the test set. w/ denotes model using pre-trained embedding and w/o denotes model without a particular pre-trained embeddings. The proposed model and its variants is compared with baseline model (CNN-RNN).

Method	BLEU-1	BLEU-2	BLEU-3	BLEU-4	C	M	R
Baseline [82]	33.84	21.11	15.15	11.46	60.33	16.46	32.23
Ours [depth=1, w/ Glove]	33.32	20.39	14.54	11.00	53.29	16.31	31.54
Ours [depth=1, w/ RadGlove]	34.69	20.28	13.71	9.71	42.44	16.20	31.28
Ours [depth=2, w/o Glove]	35.49	21.24	14.64	10.67	49.86	16.52	31.66
Ours [depth=2, w/ Glove]	35.45	21.50	14.99	11.08	60.08	16.94	32.06
Ours [depth=2, w/ RadGlove]	35.74	22.67	16.58	**12.85**	68.23	17.24	32.53
Ours [depth=3, w/o Glove]	35.90	22.23	16.08	12.48	67.07	16.74	32.44
Ours [depth=3, w/ Glove]	36.48	22.78	16.50	12.70	73.31	17.21	33.21
Ours [depth=3, w/ RadGlove]	**36.80**	**22.85**	**16.82**	12.50	**75.89**	**17.68**	**33.39**

Table 3 Experimental results on generating radiology findings from abnormal medical images in terms of BLEU-n (n=1,2,3,4), CIDEr (C), METEOR (M) and ROUGE (R) scores on the test set. w/ denotes model using pre-trained embedding and w/o denotes model without a particular pre-trained embeddings. The proposed model and its variants is compared with baseline model (CNN-RNN).

Method	BLEU-1	BLEU-2	BLEU-3	BLEU-4	C	M	R
Baseline [82]	27.07	14.92	9.07	**5.79**	12.02	12.66	24.47
Ours [depth=1, w/ Glove]	25.00	13.67	8.55	5.63	10.63	11.72	23.10
Ours [depth=1, w/ RadGlove]	21.17	12.15	8.04	5.57	15.93	12.24	**24.82**
Ours [depth=2, w/o Glove]	26.05	13.49	7.99	5.02	12.85	11.35	21.74
Ours [depth=2, w/ Glove]	25.45	13.08	7.78	5.10	13.61	11.54	22.12
Ours [depth=2, w/ RadGlove]	**30.62**	**16.04**	**9.24**	5.63	13.50	**13.05**	23.23
Ours [depth=3, w/o Glove]	27.48	13.63	7.34	4.30	9.03	12.08	22.42
Ours [depth=3, w/ Glove]	24.08	12.28	7.04	4.46	10.44	10.98	21.10
Ours [depth=3, w/ RadGlove]	23.07	11.86	7.05	4.75	**19.78**	11.11	23.15

Table 4 Experimental results on summarising normal radiology findings in terms of ROUGE-1, ROUGE-2, and ROUGE-L scores on the test set. w/ denotes model using pre-trained embedding and w/o denotes model without a particular pre-trained embeddings. The proposed model and its variants is compared with baseline model (CNN-RNN).

Method	ROUGE-1	ROUGE-2	ROUGE-L
Baseline [82]	46.58	24.89	46.33
Ours [depth=1, w/ Glove]	49.62	27.14	49.28
Ours [depth=1, w/ RadGlove]	50.04	27.92	49.68
Ours [depth=2, w/o Glove]	49.73	27.57	49.44
Ours [depth=2, w/ Glove]	**50.79**	27.38	**50.29**
Ours [depth=2, w/ RadGlove]	47.50	26.34	47.20
Ours [depth=3, w/o Glove]	48.89	**29.86**	48.57
Ours [depth=3, w/ Glove]	49.66	28.33	49.25
Ours [depth=3, w/ RadGlove]	50.34	29.66	50.07

Table 5 Experimental results on summarising abnormal radiology findings in terms of ROUGE-1, ROUGE-2, and ROUGE-L scores on the test set. w/ denotes model using pre-trained embedding and w/o denotes model without a particular pre-trained embeddings. The proposed model and its variants is compared with baseline model (CNN-RNN).

Method	ROUGE-1	ROUGE-2	ROUGE-L
Baseline [82]	8.43	1.15	8.03
Ours [depth=1, w/ Glove]	10.04	2.05	9.65
Ours [depth=1, w/ RadGlove]	6.35	0.96	5.93
Ours [depth=2, w/o Glove]	9.75	1.67	9.28
Ours [depth=2, w/ Glove]	8.81	1.24	8.49
Ours [depth=2, w/ RadGlove]	**10.47**	**2.23**	**9.91**
Ours [depth=3, w/o Glove]	6.43	1.11	6.31
Ours [depth=3, w/ Glove]	7.92	0.60	7.43
Ours [depth=3, w/ RadGlove]	8.65	1.04	8.20

Table 6 Top 15 templates (decreasing order of their frequency) in the impression of normal radiology reports which means the study is *normal*.

1	No acute cardiopulmonary abnormality.
2	No acute cardiopulmonary findings.
3	No acute cardiopulmonary disease.
4	No acute cardiopulmonary abnormalities.
5	No active disease.
6	No acute disease.
7	No acute cardiopulmonary process.
8	No acute findings.
9	No acute radiographic cardiopulmonary process.
10	Normal chest.
11	No evidence of active disease.
12	No acute pulmonary disease.
13	No evidence of active disease.
14	No acute abnormality.
15	Negative for a acute abnormality.

Table 7 Sample impression section of representative abnormal reports which mean study is *Positive*. XXXX denotes words removed during the de-identification process, resulting in some keywords missing in the report.

1	1. Bullous emphysema and interstitial fibrosis. 2. Probably scarring in the left apex, although difficult to exclude a cavitary lesion. 3. Opacities in the bilateral upper lobes could represent scarring, however the absence of comparison exam, recommend short interval followup radiograph or CT thorax to document resolution.
2	Increased size of density in the left cardiophrenic XXXX. Primary differential considerations include increased size of prominent epicardial fat, pericardial mass, pleural mass or cardiac aneurysm. CT chest with contrast is recommended. These findings and recommendations were discussed XXXX. XXXX by Dr. XXXX XXXX telephone at XXXX p.m. XXXX/XXXX. Dr. XXXX technologist receipt of the results.
3	Stable cardiomegaly. Improved aeration of lung bases with persistent left basilar effusion. Prominent interstitium, possibly due to mild volume overload.

6 Qualitative Results

In this section, we first measure the quality of generated findings and impression sections with their reference counterpart. We also check few random samples in our dataset to check where model is doing good, where model is doing bad, and what is model missing.

6.1 Analysis of generated text

We can manually inspect the quality of generated radiology report in the form of findings and impression section by our model. However, it is not feasible to do manual evaluation on an entire test set. In order to measure the quality of the generated text, the concept of *diversity* has been explored and it has been found that improving diversity of the generated text leads to more human-like text [64,84,85]. Few metrics have been proposed along with standard evaluation metrics that measures the quality of generated captions.

- *vocabulary size ratio*: In this, we calculate the ratio of the number of unique words in the generated text to the number of unique words in the reference text. A higher value indicates that model considers most of words in the reference text during text generation, helping model to have diversity in the generated text. A lower value indicates that method has learnt to do modelling of the most frequent words, ignoring rare words which may be useful in certain applications, such as medical report generation.
- *Novelty*: It is the percentage of generated captions where exact duplicates are not found in the training set. A higher value indicates that model has capability to detect novel objects, its properties, and have ability to generate novel captions.
- *Diversity*: It is the percentage of distinct captions (where duplicates count as a single distinct caption) out of the total number of generated captions within the test set. If out of N generated captions, all captions are distinct, it indicates that model is able to generate diverse captions. On the other hand, if value is lower, it indicates that model has learnt the most frequent templates in the training set, which is one of the problem of current language models, and is generating those learnt templates on the test set.

Results of the metrics that measure the quality of the generated captions are shown Table 8. We can see that for a radiology report, the average length of *findings* is quite higher compared to the average length of the *impression* section. The diversity of findings is 18.23% and for impression is 20.08%, which indicates that most of the sentences in the entire IU-CXR dataset are repetitive.

We also provide text analysis by comparing the generated findings and impression with their reference counterparts for the best model configurations. Table 9 shows results of comparing generated findings and impression by the *normal-d3-radglove* model, which is the best model configuration for generating normal radiology findings as evident from Table 2. Taking a closer look to these numbers, we can see that there are 508 unique tokens in reference findings for the test set. On the other hand, the findings generated by the model contains only 116 unique tokens. Apart from this, there is a huge gap in terms of diversity in reference text and the generated

Table 8 Analysis of the complete IU-CXR dataset.

Total images	6461
Total sentences in findings	29633
Average sentence length findings	30.88
Vocab size: Findings	1687
Unique sentences in findings	5405
Diversity in findings	18.23%
Total sentences in impression	6462
Average sentence length impression	8.64
Vocab size: Impression	1261
Unique sentences in impression	1298
Diversity in impression	20.08%

Table 9 Analysis of generated findings and impression by the *normal-d3-radglove* and *abnormal-d2-radglove* models on the test set of the IU-CXR dataset. We did analysis based on the best model configuration for normal (N) and abnormal (A) findings generation respectively.

Criteria	**N**	**A**
Unique tokens in reference findings	508	583
Unique tokens in reference impression	221	425
Diversity in reference findings	52.22%	81.76
Diversity in reference impression	34.80%	95.48%
Unique tokens in predicted findings	116	347
Unique tokens in predicted impression	15	166
Diversity in predicted findings	10.48%	60.64%
Diversity in predicted impression	4.00%	50.80%
Novelty in predicted findings	9.49%	17.24%
Novelty in predicted impressions	21.20%	48.00%

text. In terms of *novelty*, the predicted impressions have novel sentences that are not seen in the reference text during training, indicating that model is able to generate novel sentences during inferencing.

Table 9 also compares findings and impression generated by the *normal-d3-radglove* and *abnormal-d2-radglove* models, which are the best configuration for generating normal and abnormal findings respectively. In terms of vocabulary size and diversity, the abnormal findings generator provides more diverse findings and impression. On comparing results in Table 9, we can say that the findings generation module and summarisation module for abnormal images use bigger vocabulary size, is more diverse and novel.

To see model's capability in generating normal findings, we did analysis of the generated sentences by the model. The top-10 most frequent sentences in reference findings and the predicted findings are shown in Table 10. The sentences in reference findings have smaller in length, whereas the predicted sentences are longer, indicating model's ability to compose complex and longer sentences.

The top-10 most frequent sentences in reference abnormal findings and predicted abnormal findings is shown

Table 10 Top 10 sentences in reference findings and predicted findings by the *normal-d3-radglove* model for normal findings generation.

#	**Reference**	**Predicted**
1	The lungs are clear	The lungs are clear
2	Lungs are clear	Cardiomediastinum silhouette is unremarkable
3	The heart is normal in size	Visualised osseous structures of thorax are without acute abnormality
4	The mediastinum is unremarkable	The lungs are clear bilaterally
5	No pneumothorax or pleural effusion	Specifically no evidence of focal consolidation, pnemothorax or pleural effusion
6	Both lungs are clear and expanded	The cardiomediastinal silhouette is within normal limits for size and contour
7	Heart and mediastinum normal	The heart is normal in size
8	No pneumothorax	The mediastinum is unremarkable
9	There is no pleural effusion or pneumothorax	The lungs are normally inflated without evidence of focal airspace disease, pleural effusion, or pneumothorax
10	Heart size normal	Osseous structures are within normal limits for patient age

Table 11 Top 10 sentences in reference findings and predicted findings by the *abnormal-d2-radglove* model for abnormal findings generation.

#	**Reference**	**Predicted**
1	No pneumothorax	The heart is normal in size
2	The heart is normal in size	No pneumothorax
3	Heart size normal	The mediastinum is stable
4	No pleural effusion or pneumothorax	The mediastinum is unremarkable
5	Heart size is normal	The cardiomediastinal silhouette is unremarkable
6	Low lung volumes	No acute osseous abnormalities identified
7	No pneumothorax or large pleural effusion	There is no pleural effusion or pneumothorax
8	No focal infiltrates	The heart size is normal
9	The mediastinum is unremarkable	There is no pleural effusion
10	There is no pneumothorax	No pleural effusion or pneumothorax

in Table 11. Although, the table compares reference text with the generated text for abnormal reports, we can see that most frequent sentences shows normal studies. This is because when writing abnormal reports, radiologists provide detailed description about both normal regions and abnormalities present in a chest X-ray.

6.2 Where models are good and bad at?

In order to check where our best configured models are doing good and where they are performing badly, we took representative samples for each model configuration of both normal and abnormal radiology findings and impression modules. Figure 4 shows comparison of baseline model with the proposed model in generating normal findings and impression section for a given chest X-ray, when compared to the ground truth report. On seeing the first example, though both the proposed model and the baseline model provide relevant details in findings, findings generated by the proposed model provide more details such as *focal consolidation* and *osseous structures*. The impression section for both proposed and baseline model are semantically similar, concluding a negative study. In the second example, we can find *scattered calcifications are noted, compatible with prior granulomatous disease* in the ground truth findings, which indicates that radiologist have access to previous study and compared with it to find progression of disease. Both the baseline and the proposed model miss this critical information. The ground truth findings of third example mentions *surgical clips* and *background of marked centrilobular emphysema*, which baseline and the proposed model clearly miss these critical information. Since, there are few example in the training set that shows surgical clips, it is challenging for the model to learn for such a small-scale dataset.

Figure 5 shows qualitative results of the proposed model in generating abnormal findings and impression, when compared to ground truth and the baseline model. In the first case, the ground truth findings shows *bilateral interstitial opacities* as an abnormality. The baseline model is missing this critical information, but also includes inaccurate or spurious information such as *the aorta is atherosclerotic*, which indicates that the baseline model generates inaccurate or spurious information. On the other hand, the proposed model is able to highlight *nodular opacity* as given in the ground truth findings. The generated impression section includes *num mm nodular opacity*. This is because the all numbers are mapped to *num* token due to model's incapability to do morphological analysis of lesions. In the second example, again the proposed model is able to correctly identify *low lung volumes*, whereas the baseline model shows normal study. Another notable finding is that generated findings are sometimes redundant, where the model is repetitive in generating most common normal sentences. We also find grammatical errors as well as misplacement of punctuation, which can completely change the meaning of radiology reports. In the last example of Figure 5, there are two abnormalities: *low lung volumes* and *bibasilar atelectasis versus scarring*. Rest everything is normal in the chest X-ray. The baseline model generates inaccurate abnormality in the form *the mediastinum is stable* and also concludes the study as normal. On the other hand, the proposed model, though is able to correctly identify abnormality *bibasilar airspace opacities*, but also generates spurious information in the form of *the cardiac silhouette is enlarged* and *pleural effusion*.

7 Discussion

The qualitative and quantitative results shows that deep learning has potential to automatically generate radiology reports from medical images. With the increasing demand of imaging and improvement in imaging modalities, the role of radiologists is invariably expanding. Artificial intelligence based clinical decision support systems, such as automatic generation of radiology reports, will allow radiologists to expand their roles including communication with clinicians, leading interventional procedures, conducting quality assurance, and improving healthcare quality. AI has the potential to develop systems that can automate routine, tedious, and boring tasks in the healthcare domain, however, these systems do not have the ability to engage in complex conversation with humans or have empathy similar to humans. Hence, doctors and radiologists will continue to hold an influential and irreplaceable role in patient care, while AI can help enhance such a position. In future, radiologists will help in integrating information from imaging to clinical data as well as offering valuable insights to other medical professionals in the diagnosis and individualised management of patients.

8 Challenges and Future Work

In this section, we provide limitations that need to be addressed to have reliable automated systems for radiology report generation. Based on these limitations, we provide future research directions that can help towards generating robust, diverse, and clinically accurate radiology reports.

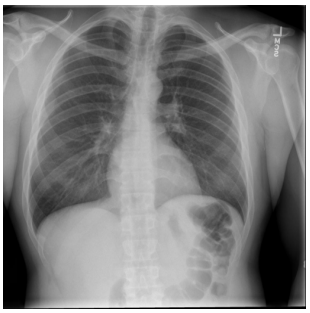

Ground Truth:
Findings:The heart is normal size. The mediastinum is unremarkable. There is no pleural effusion, pneumothorax, or focal airspace disease. The XXXX are unremarkable.
Impression: No acute cardiopulmonary abnormality.

Baseline:
Findings: Lungs are clear. There is no pneumothorax or pleural effusion. The heart and mediastinum are within normal limits. Bony structures are intact.
Impression: No evidence of acute cardiopulmonary disease.

Proposed Model:
Findings: The lungs are clear bilaterally. Specifically no evidence of focal consolidation, pneumothorax or pleural effusion. Cardio mediastinal silhouette is unremarkable. Visualized osseous structures of the thorax are without acute abnormality.
Impression: No evidence of acute cardiopulmonary disease.

Ground Truth:
Findings: The heart is normal in size and contour. Scattered calcifications are noted, compatible with prior granulomatous disease. The lungs are clear, without evidence of infiltrate. There is no pneumothorax or effusion.
Impression: No acute cardiopulmonary disease.

Baseline:
Findings: Heart size and pulmonary vascularity appear within normal limits. The lungs are free of focal airspace disease. No pleural effusion or pneumothorax is seen.
Impression: Normal chest.

Proposed Model:
Findings: Heart size within normal limits. Stable mediastinal and hilar contours. No focal alveolar consolidation. No definite pleural effusion seen. No typical findings of pulmonary edema.
Impression: No acute cardiopulmonary findings.

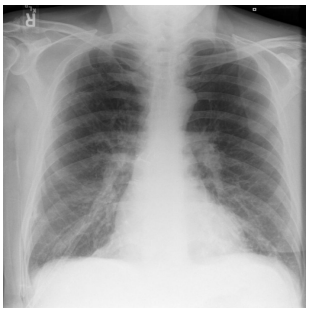

Ground Truth:
Findings: The XXXX examination consists of frontal and lateral radiographs of the chest. Sternotomy XXXX and surgical clips are again seen. The cardiomediastinal contours are unchanged. There is a background of marked centrilobular emphysema. Streaky opacities in the lung bases may represent atelectasis or scarring. There is no consolidation, pleural effusion or pneumothorax.
Impression: No evidence of acute cardiopulmonary disease or significant interval change.

Baseline:
Findings: The heart size and pulmonary vascularity appear within normal limits the lungs are free of focal airspace disease no pleural effusion or pneumothorax is seen.
Impression: No evidence of acute cardiopulmonary disease.

Proposed Model:
Findings: The heart size and pulmonary vascularity appear within normal limits the lungs are free of focal airspace disease no pleural effusion or pneumothorax is seen.
Impression: No evidence of acute cardiopulmonary disease.

Fig. 4 Qualitative examples of generating *normal findings and impression* sections from chest X-rays. First column denotes chest X-ray given as input to the proposed model. Second column highlights ground truth findings and impression section for the given chest X-ray. Third column denotes generated findings and impression by the baseline model, and the last column denotes findings and impression generated by the proposed model. XXXX denotes keywords that are removed during data de-identification. Note: The generated text is in lower case. We changed first letter of each sentence to upper case to improve its readability.

8.1 Challenges

Although qualitative and quantitative results are encouraging, there are various challenges that need to be alleviated before these systems can be deployed in real clinical settings. Various challenges are:

Error propagation: Since the proposed methodology have a sequential processing pipeline, an error in the image classification module can be propagated to generation module. Similarly, an error in generation module can be propagated to the summarisation module. Hence,

No background information: In actual radiology practice, background information in the form of *comparison* and *indication* are available. Due to data anonymisation, most of the background information is lost in the dataset curation process. This limits model's capability to use background information.

No annotated bounding boxes: The generic image captioning models improved their performance by using object detection methods based on the annotated

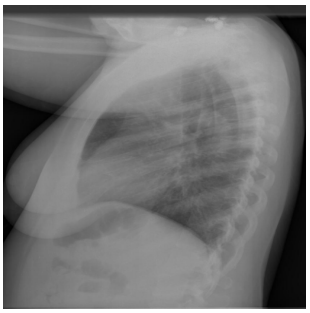	**Ground Truth**: **Findings**: Stable heart size. Diffuse bilateral interstitial opacities. No pneumothorax. No effusions. No acute bony abnormalities. **Impression**: Stable bilateral interstitial opacities, could represent scarring or infiltrate. CT may be helpful to further characterize.	**Baseline**: **Findings**: The heart is normal in size. The mediastinum is stable. The aorta is atherosclerotic. There are low lung volumes. No focal consolidation, pneumothorax or large pleural effusion. **Impression**: No acute cardiopulmonary abnormality.	**Proposed Model**: **Findings**: There is a num mm nodular opacity in the right midlung. No pneumothorax no pleural effusion. No acute bony abnormality. **Impression**: num mm nodular opacity in the right midlung.
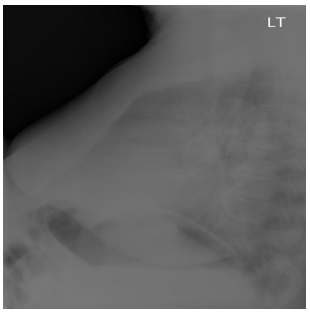	**Ground Truth**: **Findings**: Lung volumes are low. No focal infiltrates. Pulmonary XXXX are normal. **Impression**: XXXX change. Hypoinflation with no visible active cardiopulmonary disease.	**Baseline**: **Findings**: The heart is normal in size. The mediastinum is stable. The aorta is atherosclerotic. There are low lung volumes. No focal consolidation pneumothorax or large pleural effusion. **Impression**: No acute cardiopulmonary abnormality.	**Proposed Model**: **Findings**: Low lung volumes bilaterally with central bronchovascular crowding. Without focal consolidation pleural effusion or pneumothoraces. Cardiomediastinal silhouette is within normal limits. Degenerative changes of the thoracic spine. **Impression**: No radiographic evidence of acute cardiopulmonary disease.
	**Ground Truth**: **Findings**: Low lung volumes. Bibasilar atelectasis versus scarring. Stable left abdominal surgical clips. The heart size and mediastinal silhouette are within normal limits for contour. No pneumothorax or pleural effusions. The XXXX are intact. **Impression**: Low lung volumes. Bibasilar atelectasis versus scarring.	**Baseline**: **Findings**: The heart is normal in size. The mediastinum is stable. The lungs are clear. **Impression**: No evidence of acute cardiopulmonary process.	**Proposed Model**: **Findings**: The cardiac silhouette is enlarged. There are bibasilar airspace opacities left greater than right with small right pleural effusion. No pneumothorax. **Impression**: Bibasilar airspace opacities left greater than right with small right pleural effusion. No pneumothorax .

Fig. 5 Qualitative examples of generating *abnormal findings and impression* sections from chest X-rays. First column denotes chest X-ray given as input to the proposed model. Second column highlights ground truth findings and impression section for the given chest X-ray. Third column denotes generated findings and impression by the baseline model, and the last column denotes findings and impression generated by the proposed model. XXXX denotes keywords that are removed during data de-identification. Note: The generated text is in lower case. We changed first letter of each sentence to upper case to improve its readability.

bounding boxes on objects and their relationships. This can be used to ensure that the captioning model pays attention to all the detected objects and their relationships within a scene. On the other hand, medical multimodal datasets lack manually annotated bounding boxes for normal or abnormal regions, making it difficult for the CNN model to get fine-grained features tailored at various medical concepts.

Examining the suitability of NLG metrics for radiology report generation evaluation: In order to evaluate the effectiveness of proposed models for radiology report generation, automated evaluation methods are used. Though qualitative human evaluation is possible on fewer samples for error analysis, but manual evaluation on thousands of medical images is not possible. This led to the need of automated methods for radiology report generation using natural language generation evaluation metrics, mostly inspired from the machine translation and summarisation research. To the best of our knowledge, there is no study undertaken to examine the suitability of automated evaluation metrics for the radiology report generation task. There is no study which reflects to what extent, higher values in terms of evaluation metric highlight better radiology report or do higher values of evaluation metric reflects grammatically correct, diverse, fluent, and clinically accurate report.

8.2 Future Work

Based on our text analysis of the generated text, we observe that decoder is generating the most frequent sentences due to limitations of language modelling. To overcome this, in our future work, we aim to use better language models including ELMo [86],transfomer [87], and Bidirectional Encoder Representations from Transformers (BERT) [88]. These state-of-the-art language models have capability in interpreting context, polysemous words, nuances and meanings of the sentences.

9 Conclusions

In this paper, we present a novel *show, tell and summarise* model for radiology report generation from chest X-rays. The proposed model is capable of generating findings and impression section separately, overcoming the limitations of previous studies. The proposed model first classifies an input chest X-ray as normal or abnormal and then respective findings generation module generates the findings. The generated findings are summarised to get an impression section. The proposed model can be a part of clinical decision support systems (CDSS), which augment radiologists by providing "second opinion", providing draft radiology report, and expedite the clinical workflow. These CDSS systems have potential to fasten clinical workflow, in turn providing early detection of diseases, saving human lives.

Acknowledgements This work is supported by an international Macquarie University Research Excellence Scholarship and the Data61 CSIRO top-up scholarship. This research was undertaken with the assistance of resources from the National Computational Infrastructure (NCI) and the CSIRO Bracewell GPU clusters, supported by the Australian Government.

Conflict of Interest: There are no conflicts of interests in this work.

References

1. Lewis, S.J., Gandomkar, Z., Brennan, P.C.: Artificial intelligence in medical imaging practice: looking to the future. Journal of Medical Radiation Sciences **66**(4), 292–295 (2019)
2. Demner-Fushman, D., Kohli, M.D., Rosenman, M.B., Shooshan, S.E., Rodriguez, L., Antani, S., Thoma, G.R., McDonald, C.J.: Preparing a collection of radiology examinations for distribution and retrieval. Journal of the American Medical Informatics Association **23**(2), 304–310 (2016)
3. Kisilev, P., Walach, E., Barkan, E., Ophir, B., Alpert, S., Hashoul, S.Y.: From medical image to automatic medical report generation. IBM Journal of Research and Development **59**(2/3), 2:1–2:7 (2015)
4. Kisilev, P., Sason, E., Barkan, E., Hashoul, S.: Medical image description using multi-task-loss cnn. In: G. Carneiro, D. Mateus, L. Peter, A. Bradley, J.M.R.S. Tavares, V. Belagiannis, J.P. Papa, J.C. Nascimento, M. Loog, Z. Lu, J.S. Cardoso, J. Cornebise (eds.) Deep Learning and Data Labeling for Medical Applications, pp. 121–129. Springer International Publishing (2016)
5. Jing, B., Xie, P., Xing, E.: On the Automatic Generation of Medical Imaging Reports. In: Proceedings of the 56th Annual Meeting of the Association for Computational Linguistics (Volume 1: Long Papers), pp. 2577–2586. Association for Computational Linguistics (2018)
6. Yin, C., Qian, B., Wei, J., Li, X., Zhang, X., Li, Y., Zheng, Q.: Automatic generation of medical imaging diagnostic report with hierarchical recurrent neural network. In: 2019 IEEE International Conference on Data Mining (ICDM), pp. 728–737 (2019)
7. Jing, B., Wang, Z., Xing, E.: Show, describe and conclude: On exploiting the structure information of chest x-ray reports. In: Proceedings of the 57th Annual Meeting of the Association for Computational Linguistics, pp. 6570–6580. Association for Computational Linguistics, Florence, Italy (2019)
8. Kolen, J.F., Kremer, S.C.: Gradient Flow in Recurrent Nets: The Difficulty of Learning LongTerm Dependencies, pp. 237–243. IEEE Computer Society (2001)
9. Vinyals, O., Toshev, A., Bengio, S., Erhan, D.: Show and tell: Lessons learned from the 2015 mscoco image captioning challenge. IEEE Transactions on Pattern Analysis and Machine Intelligence **39**(4), 652–663 (2017)
10. Goodfellow, I., Bengio, Y., Courville, A.: Deep Learning. The MIT Press (2016)
11. Lee, L.I.T., Kanthasamy, S., Ayyalaraju, R.S., Ganatra, R.: The current state of artificial intelligence in medical imaging and nuclear medicine. BJR—Open **1**(1), 20190037 (2019)
12. Wang, X., Peng, Y., Lu, L., Lu, Z., Bagheri, M., Summers, R.M.: ChestX-Ray8: Hospital-scale chest X-Ray database and benchmarks on weakly-supervised classification and localization of common thorax diseases. In: IEEE Conference on Computer Vision and Pattern Recognition, pp. 3462–3471. Hawaii, United States (2017)
13. Bustos, A., Pertusa, A., Salinas, J., de la Iglesia-Vayá, M.: Padchest: A large chest x-ray image dataset with multi-label annotated reports. arXiv:1901.07441 (2019)
14. Johnson, A.E.W., Pollard, T.J., Berkowitz, S.J., Greenbaum, N.R., Lungren, M.P., Deng, C.y., Mark, R.G., Horng, S.: Mimic-cxr, a de-identified publicly available database of chest radiographs with free-text reports. Scientific Data **6**(1), 317 (2019)
15. Irvin, J., Rajpurkar, P., Ko, M., Yu, Y., Ciurea-Ilcus, S., Chute, C., Marklund, H., Haghgoo, B., Ball, R.L., Shpanskaya, K.S., Seekins, J., Mong, D.A., Halabi, S.S., Sandberg, J.K., Jones, R., Larson, D.B., Langlotz, C.P., Patel, B.N., Lungren, M.P., Ng, A.Y.: Chexpert: A large chest radiograph dataset with uncertainty labels and expert comparison. In: The Thirty-Third AAAI Conference on Artificial Intelligence, AAAI 2019, The Thirty-First Innovative Applications of Artificial Intelligence Conference, IAAI 2019, The Ninth AAAI Symposium on Educational Advances in Artificial Intelligence, EAAI 2019, Honolulu, Hawaii, USA, January 27 - February 1, 2019, pp. 590–597. AAAI Press (2019)
16. Krizhevsky, A., Sutskever, I., Hinton, G.E.: Imagenet classification with deep convolutional neural networks.

In: F. Pereira, C.J.C. Burges, L. Bottou, K.Q. Weinberger (eds.) Advances in Neural Information Processing Systems, pp. 1097–1105. Curran Associates, Inc. (2012)
17. Szegedy, C., Vanhoucke, V., Ioffe, S., Shlens, J., Wojna, Z.: Rethinking the Inception Architecture for Computer Vision. In: IEEE Conference on Computer Vision and Pattern Recognition, pp. 2818–2826 (2016)
18. He, K., Zhang, X., Ren, S., Sun, J.: Deep residual learning for image recognition. In: 2016 IEEE Conference on Computer Vision and Pattern Recognition, pp. 770–778 (2016)
19. Gündel, S., Grbic, S., Georgescu, B., Liu, S., Maier, A., Comaniciu, D.: Learning to recognize abnormalities in chest x-rays with location-aware dense networks. In: R. Vera-Rodriguez, J. Fierrez, A. Morales (eds.) Progress in Pattern Recognition, Image Analysis, Computer Vision, and Applications, pp. 757–765. Springer International Publishing (2019)
20. Rajpurkar, P., Irvin, J., Zhu, K., Yang, B., Mehta, H., Duan, T., Ding, D., Bagul, A., Langlotz, C., Shpanskaya, K., Lungren, M.P., Ng, A.Y.: Chexnet: Radiologist-level pneumonia detection on chest x-rays with deep learning (2017)
21. Rajpurkar, P., Irvin, J., Ball, R.L., Zhu, K., Yang, B., Mehta, H., Duan, T., Ding, D., Bagul, A., Langlotz, C.P., Patel, B.N., Yeom, K.W., Shpanskaya, K., Blankenberg, F.G., Seekins, J., Amrhein, T.J., Mong, D.A., Halabi, S.S., Zucker, E.J., Ng, A.Y., Lungren, M.P.: Deep learning for chest radiograph diagnosis: A retrospective comparison of the chexnext algorithm to practicing radiologists. PLOS Medicine **15**(11), 1–17 (2018)
22. Baltruschat, I.M., Nickisch, H., Grass, M., Knopp, T., Saalbach, A.: Comparison of deep learning approaches for multi-label chest x-ray classification. Scientific Reports **9**(1), 6381 (2019)
23. Yao, L., Poblenz, E., Dagunts, D., Covington, B., Bernard, D., Lyman, K.: Learning to diagnose from scratch by exploiting dependencies among labels. CoRR **abs/1710.10501** (2017)
24. Singh, S., Ho-Shon, K., Karimi, S., Hamey, L.: Modality classification and concept detection in medical images using deep transfer learning. In: 2018 International Conference on Image and Vision Computing New Zealand (IVCNZ), pp. 1–9 (2018)
25. Wang, W., Liang, D., Chen, Q., Iwamoto, Y., Han, X.H., Zhang, Q., Hu, H., Lin, L., Chen, Y.W.: Medical Image Classification Using Deep Learning, pp. 33–51. Springer International Publishing (2020)
26. Yadav, S.S., Jadhav, S.M.: Deep convolutional neural network based medical image classification for disease diagnosis. Journal of Big Data **6**(1), 113 (2019)
27. Zhang, J., Xie, Y., Wu, Q., Xia, Y.: Medical image classification using synergic deep learning. Medical Image Analysis **54**, 10 – 19 (2019)
28. Kumar, A., Kim, J., Lyndon, D., Fulham, M., Feng, D.: An ensemble of fine-tuned convolutional neural networks for medical image classification. IEEE Journal of Biomedical and Health Informatics **21**(1), 31–40 (2017)
29. Faes, L., Wagner, S.K., Fu, D.J., Liu, X., Korot, E., Ledsam, J.R., Back, T., Chopra, R., Pontikos, N., Kern, C., Moraes, G., Schmid, M.K., Sim, D., Balaskas, K., Bachmann, L.M., Denniston, A.K., Keane, P.A.: Automated deep learning design for medical image classification by health-care professionals with no coding experience: a feasibility study. The Lancet Digital Health **1**(5), e232 – e242 (2019)
30. Hossain, M.Z., Sohel, F., Shiratuddin, M.F., Laga, H.: A comprehensive survey of deep learning for image captioning. ACM Computing Surveys **51**(6), 118:1–118:36 (2019)
31. Farhadi, A., Hejrati, M., Sadeghi, M.A., Young, P., Rashtchian, C., Hockenmaier, J., Forsyth, D.: Every picture tells a story: Generating sentences from images. In: K. Daniilidis, P. Maragos, N. Paragios (eds.) Computer Vision – ECCV 2010, pp. 15–29. Springer Berlin Heidelberg, Berlin, Heidelberg (2010)
32. Li, S., Kulkarni, G., Berg, T.L., Berg, A.C., Choi, Y.: Composing simple image descriptions using web-scale n-grams. In: Proceedings of the Fifteenth Conference on Computational Natural Language Learning, CoNLL '11, p. 220–228. Association for Computational Linguistics, USA (2011)
33. Kulkarni, G., Premraj, V., Ordonez, V., Dhar, S., Li, S., Choi, Y., Berg, A.C., Berg, T.L.: Babytalk: Understanding and generating simple image descriptions. IEEE Transactions on Pattern Analysis and Machine Intelligence **35**(12), 2891–2903 (2013)
34. Hodosh, M., Young, P., Hockenmaier, J.: Framing image description as a ranking task: Data, models and evaluation metrics. J. Artif. Int. Res. **47**(1), 853–899 (2013)
35. Mason, R., Charniak, E.: Nonparametric method for data-driven image captioning. In: Proceedings of the 52nd Annual Meeting of the Association for Computational Linguistics (Volume 2: Short Papers), pp. 592–598. Association for Computational Linguistics, Baltimore, Maryland (2014)
36. Ordonez, V., Kulkarni, G., Berg, T.L.: Im2text: Describing images using 1 million captioned photographs. In: J. Shawe-Taylor, R.S. Zemel, P.L. Bartlett, F. Pereira, K.Q. Weinberger (eds.) Advances in Neural Information Processing Systems 24, pp. 1143–1151. Curran Associates, Inc. (2011)
37. Mason, R., Charniak, E.: Nonparametric method for data-driven image captioning. In: Proceedings of the 52nd Annual Meeting of the Association for Computational Linguistics (Volume 2: Short Papers), pp. 592–598. Association for Computational Linguistics (2014)
38. Kiros, R., Salakhutdinov, R., Zemel, R.: Multimodal neural language models. In: E.P. Xing, T. Jebara (eds.) Proceedings of the 31st International Conference on Machine Learning, *Proceedings of Machine Learning Research*, vol. 32, pp. 595–603. PMLR, Bejing, China (2014)
39. Karpathy, A., Fei-Fei, L.: Deep visual-semantic alignments for generating image descriptions. IEEE Transactions on Pattern Analysis and Machine Intelligence **39**(4), 664–676 (2017)
40. Xu, K., Ba, J., Kiros, R., Cho, K., Courville, A., Salakhudinov, R., Zemel, R., Bengio, Y.: Show, attend and tell: Neural image caption generation with visual attention. In: F. Bach, D. Blei (eds.) Proceedings of the 32nd International Conference on Machine Learning, *Proceedings of Machine Learning Research*, vol. 37, pp. 2048–2057. PMLR, Lille, France (2015)
41. Liu, C., Mao, J., Sha, F., Yuille, A.: Attention correctness in neural image captioning. In: Proceedings of the Thirty-First AAAI Conference on Artificial Intelligence, AAAI'17, p. 4176–4182. AAAI Press (2017)
42. You, Q., Jin, H., Wang, Z., Fang, C., Luo, J.: Image captioning with semantic attention. In: 2016 IEEE Conference on Computer Vision and Pattern Recognition (CVPR), pp. 4651–4659 (2016)
43. Anderson, P., He, X., Buehler, C., Teney, D., Johnson, M., Gould, S., Zhang, L.: Bottom-up and top-down atten-

tion for image captioning and visual question answering. In: 2018 IEEE/CVF Conference on Computer Vision and Pattern Recognition, pp. 6077–6086 (2018)
44. Krause, J., Johnson, J., Krishna, R., Fei-Fei, L.: A hierarchical approach for generating descriptive image paragraphs. In: 2017 IEEE Conference on Computer Vision and Pattern Recognition, pp. 3337–3345 (2017)
45. Johnson, J., Karpathy, A., Fei-Fei, L.: DenseCap: Fully Convolutional Localization Networks for Dense Captioning. In: 2016 IEEE Conference on Computer Vision and Pattern Recognition, pp. 4565–4574 (2016)
46. Xue, Y., Xu, T., Rodney Long, L., Xue, Z., Antani, S., Thoma, G.R., Huang, X.: Multimodal recurrent model with attention for automated radiology report generation. In: A.F. Frangi, J.A. Schnabel, C. Davatzikos, C. Alberola-López, G. Fichtinger (eds.) Medical Image Computing and Computer Assisted Intervention – MICCAI 2018, pp. 457–466. Springer International Publishing (2018)
47. Xiong, Y., Du, B., Yan, P.: Reinforced transformer for medical image captioning. In: H.I. Suk, M. Liu, P. Yan, C. Lian (eds.) Machine Learning in Medical Imaging, pp. 673–680. Springer International Publishing (2019)
48. Schlegl, T., Waldstein, S.M., Vogl, W.D., Schmidt-Erfurth, U., Langs, G.: Predicting semantic descriptions from medical images with convolutional neural networks. In: S. Ourselin, D.C. Alexander, C.F. Westin, M.J. Cardoso (eds.) Information Processing in Medical Imaging, pp. 437–448. Springer International Publishing, Cham (2015)
49. Shin, H.C., Lu, L., Kim, L., Seff, A., Yao, J., Summers, R.M.: Interleaved text/image deep mining on a large-scale radiology database for automated image interpretation. Journal of Machine Learning Research **17**(107), 1–31 (2016)
50. Shin, H., Roberts, K., Lu, L., Demner-Fushman, D., Yao, J., Summers, R.M.: Learning to read chest x-rays: Recurrent neural cascade model for automated image annotation. In: 2016 IEEE Conference on Computer Vision and Pattern Recognition (CVPR), pp. 2497–2506 (2016). DOI 10.1109/CVPR.2016.274
51. Zhang, Z., Xie, Y., Xing, F., McGough, M., Yang, L.: MDNet: A Semantically and Visually Interpretable Medical Image Diagnosis Network. In: IEEE Conference on Computer Vision and Pattern Recognition, pp. 3549–3557. Hawaii, United States (2017)
52. Li, Y., Liang, X., Hu, Z., Xing, E.P.: Hybrid retrieval-generation reinforced agent for medical image report generation. In: S. Bengio, H. Wallach, H. Larochelle, K. Grauman, N. Cesa-Bianchi, R. Garnett (eds.) Advances in Neural Information Processing Systems 31, pp. 1530–1540. Curran Associates, Inc. (2018)
53. Zeng, X.H., Liu, B.G., Zhou, M.: Understanding and generating ultrasound image description. Journal of Computer Science and Technology **33**(5), 1086–1100 (2018)
54. Radev, D.R., Hovy, E., McKeown, K.: Introduction to the special issue on summarization. Comput. Linguist. **28**(4), 399–408 (2002)
55. Mishra, R., Bian, J., Fiszman, M., Weir, C.R., Jonnalagadda, S., Mostafa, J., Del Fiol, G.: Text summarization in the biomedical domain. J. of Biomedical Informatics **52**(C), 457–467 (2014)
56. Neto, J.L., Freitas, A.A., Kaestner, C.A.A.: Automatic text summarization using a machine learning approach. In: Proceedings of the 16th Brazilian Symposium on Artificial Intelligence: Advances in Artificial Intelligence, SBIA '02, p. 205–215. Springer-Verlag, Berlin, Heidelberg (2002)
57. Filippova, K., Altun, Y.: Overcoming the lack of parallel data in sentence compression. In: Proceedings of the 2013 Conference on Empirical Methods in Natural Language Processing, pp. 1481–1491. Association for Computational Linguistics, Seattle, Washington, USA (2013)
58. Colmenares, C.A., Litvak, M., Mantrach, A., Silvestri, F.: HEADS: Headline generation as sequence prediction using an abstract feature-rich space. In: Proceedings of the 2015 Conference of the North American Chapter of the Association for Computational Linguistics: Human Language Technologies, pp. 133–142. Association for Computational Linguistics, Denver, Colorado (2015)
59. Kryscinski, W., Keskar, N.S., McCann, B., Xiong, C., Socher, R.: Neural text summarization: A critical evaluation. In: Proceedings of the 2019 Conference on Empirical Methods in Natural Language Processing and the 9th International Joint Conference on Natural Language Processing (EMNLP-IJCNLP), pp. 540–551. Association for Computational Linguistics, Hong Kong, China (2019)
60. See, A., Liu, P.J., Manning, C.D.: Get to the point: Summarization with pointer-generator networks. In: Proceedings of the 55th Annual Meeting of the Association for Computational Linguistics (Volume 1: Long Papers), pp. 1073–1083. Association for Computational Linguistics, Vancouver, Canada (2017)
61. Tan, J., Wan, X., Xiao, J.: Abstractive document summarization with a graph-based attentional neural model. In: Proceedings of the 55th Annual Meeting of the Association for Computational Linguistics (Volume 1: Long Papers), pp. 1171–1181. Association for Computational Linguistics, Vancouver, Canada (2017)
62. Cohan, A., Dernoncourt, F., Kim, D.S., Bui, T., Kim, S., Chang, W., Goharian, N.: A discourse-aware attention model for abstractive summarization of long documents. In: Proceedings of the 2018 Conference of the North American Chapter of the Association for Computational Linguistics: Human Language Technologies, Volume 2 (Short Papers), pp. 615–621. Association for Computational Linguistics, New Orleans, Louisiana (2018)
63. Hsu, W.T., Lin, C.K., Lee, M.Y., Min, K., Tang, J., Sun, M.: A unified model for extractive and abstractive summarization using inconsistency loss. In: Proceedings of the 56th Annual Meeting of the Association for Computational Linguistics (Volume 1: Long Papers), pp. 132–141. Association for Computational Linguistics, Melbourne, Australia (2018)
64. Liu, L., Tang, J., Wan, X., Guo, Z.: Generating diverse and descriptive image captions using visual paraphrases. In: 2019 IEEE/CVF International Conference on Computer Vision (ICCV), pp. 4239–4248 (2019)
65. Gehrmann, S., Deng, Y., Rush, A.: Bottom-up abstractive summarization. In: Proceedings of the 2018 Conference on Empirical Methods in Natural Language Processing, pp. 4098–4109. Association for Computational Linguistics, Brussels, Belgium (2018)
66. Chen, Y.C., Bansal, M.: Fast abstractive summarization with reinforce-selected sentence rewriting. In: Proceedings of the 56th Annual Meeting of the Association for Computational Linguistics (Volume 1: Long Papers), pp. 675–686. Association for Computational Linguistics, Melbourne, Australia (2018)
67. Moirangthem, D.S., Lee, M.: Abstractive summarization of long texts by representing multiple compositionalities with temporal hierarchical pointer generator network. Neural Networks **124**, 1–11 (2020)

68. Deng, J., Dong, W., Socher, R., Li, L., Kai Li, Li Fei-Fei: Imagenet: A large-scale hierarchical image database. In: 2009 IEEE Conference on Computer Vision and Pattern Recognition, pp. 248–255 (2009)
69. Zhang, Y., Ding, D.Y., Qian, T., Manning, C.D., Langlotz, C.P.: Learning to summarize radiology findings. In: Proceedings of the Ninth International Workshop on Health Text Mining and Information Analysis, pp. 204–213. Association for Computational Linguistics, Brussels, Belgium (2018)
70. Bahdanau, D., Cho, K., Bengio, Y.: Neural machine translation by jointly learning to align and translate. In: 3rd International Conference on Learning Representations, ICLR 2015 ; Conference date: 07-05-2015 Through 09-05-2015 (2015)
71. Razavian, A.S., Azizpour, H., Sullivan, J., Carlsson, S.: Cnn features off-the-shelf: An astounding baseline for recognition. In: 2014 IEEE Conference on Computer Vision and Pattern Recognition Workshops, pp. 512–519 (2014)
72. Raghu, M., Zhang, C., Kleinberg, J., Bengio, S.: Transfusion: Understanding transfer learning for medical imaging. In: H. Wallach, H. Larochelle, A. Beygelzimer, F.AlcheBuc, E. Fox, R. Garnett (eds.) Advances in Neural Information Processing Systems 32, pp. 3347–3357. Curran Associates, Inc. (2019)
73. Singh, S., Karimi, S., Ho-Shon, K., Hamey, L.: From chest x-rays to radiology reports: A multimodal machine learning approach. In: 2019 Digital Image Computing: Techniques and Applications (DICTA), pp. 1–8 (2019)
74. Papineni, K., Roukos, S., Ward, T., Zhu, W.J.: BLEU: a method for automatic evaluation of machine translation. In: Proceedings of the 40th Annual Meeting of the Association for Computational Linguistics. Philadelphia, Pennsylvania, United States (2002)
75. Lin, C.Y.: ROUGE: A package for automatic evaluation of summaries. In: 42nd Annual Meeting of the Association for Computational Linguistics, pp. 1–8. Barcelona, Spain (2004)
76. Banerjee, S., Lavie, A.: METEOR: An automatic metric for MT evaluation with improved correlation with human judgments. In: Proceedings of the ACL Workshop on Intrinsic and Extrinsic Evaluation Measures for Machine Translation and/or Summarization, pp. 65–72. Ann Arbor, Michigan, United States (2005)
77. Vedantam, R., Zitnick, C.L., Parikh, D.: CIDEr: Consensus-based image description evaluation. In: IEEE Conference on Computer Vision and Pattern Recognition, pp. 4566–4575. Boston, Massachusetts, United States (2015)
78. Chen, X., Hao Fang, T.Y.L., Vedantam, R., Gupta, S., Dollár, P., Zitnick, C.L.: Microsoft COCO captions: Data collection and evaluation server. arXiv preprint arXiv:1504.00325 (2015)
79. Chollet, F., et al.: Keras. https://github.com/fchollet/keras (2015)
80. Abadi, M., Barham, P., Chen, J., Chen, Z., Davis, A., Dean, J., Devin, M., Ghemawat, S., Irving, G., Isard, M., et al.: Tensorflow: A system for large-scale machine learning. In: Proceedings of the 12th USENIX Conference on Operating Systems Design and Implementation, OSDI'16, p. 265–283. USENIX Association, USA (2016)
81. Kingma, D.P., Ba, J.: Adam: A method for stochastic optimization. In: Y. Bengio, Y. LeCun (eds.) 3rd International Conference on Learning Representations, ICLR 2015, San Diego, CA, USA, May 7-9, 2015, Conference Track Proceedings (2015)
82. Vinyals, O., Toshev, A., Bengio, S., Erhan, D.: Show and Tell: A Neural Image Caption generator. In: 2015 IEEE Conference on Computer Vision and Pattern Recognition, pp. 3156–3164 (2015)
83. Pennington, J., Socher, R., Manning, C.D.: GloVe: Global Vectors for Word Representation. In: Empirical Methods in Natural Language Processing, pp. 1532–1543. Doha, Qatar (2014)
84. Lindh, A., Ross, R.J., Mahalunkar, A., Salton, G., Kelleher, J.D.: Generating diverse and meaningful captions. In: V. Kůrková, Y. Manolopoulos, B. Hammer, L. Iliadis, I. Maglogiannis (eds.) Artificial Neural Networks and Machine Learning – ICANN 2018, pp. 176–187. Springer International Publishing (2018)
85. Deshpande, A., Aneja, J., Wang, L., Schwing, A.G., Forsyth, D.: Fast, diverse and accurate image captioning guided by part-of-speech. In: 2019 IEEE/CVF Conference on Computer Vision and Pattern Recognition (CVPR), pp. 10687–10696 (2019)
86. Peters, M., Neumann, M., Iyyer, M., Gardner, M., Clark, C., Lee, K., Zettlemoyer, L.: Deep contextualized word representations. In: Proceedings of the 2018 Conference of the North American Chapter of the Association for Computational Linguistics: Human Language Technologies, Volume 1 (Long Papers), pp. 2227–2237. Association for Computational Linguistics, New Orleans, Louisiana (2018)
87. Vaswani, A., Shazeer, N., Parmar, N., Uszkoreit, J., Jones, L., Gomez, A.N., Kaiser, L.u., Polosukhin, I.: Attention is all you need. In: I. Guyon, U.V. Luxburg, S. Bengio, H. Wallach, R. Fergus, S. Vishwanathan, R. Garnett (eds.) Advances in Neural Information Processing Systems 30, pp. 5998–6008. Curran Associates, Inc. (2017)
88. Devlin, J., Chang, M.W., Lee, K., Toutanova, K.: BERT: Pre-training of deep bidirectional transformers for language understanding. In: Proceedings of the 2019 Conference of the North American Chapter of the Association for Computational Linguistics: Human Language Technologies, Volume 1 (Long and Short Papers), pp. 4171–4186. Association for Computational Linguistics, Minneapolis, Minnesota (2019)

Figure

Click here to access/download;Figure;Block-Diagram.tif

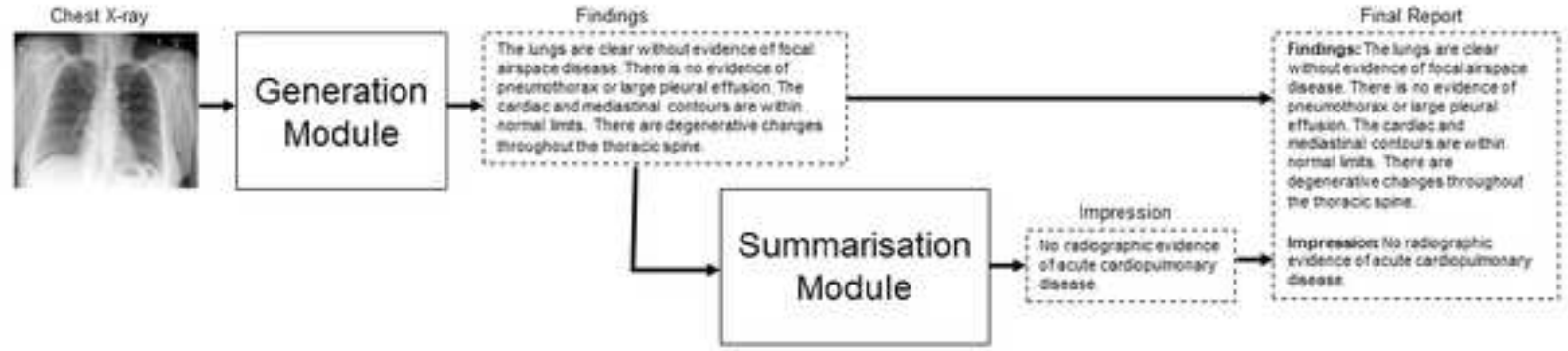

Figure

Click here to access/download;Figure;CXR1170_IM-0115-2001.png

Figure

Click here to access/download;Figure;CXR1324_IM-0209-1001.png

Figure

Click here to access/download;Figure;Show_Tell_Summarise.tiff